

# Design and Modelling of a Microfluidic Electro-Lysis Device with Controlling Plates

A. Jenkins<sup>1</sup>, C. P. Chen<sup>2</sup>, S. Spearing<sup>1</sup>, L. A. Monaco<sup>3</sup>, A. Steele<sup>4</sup>,  
and G. Flores<sup>5</sup>

<sup>1</sup>Morgan Research Corporation, Huntsville, AL

<sup>2</sup>University of Alabama in Huntsville, Huntsville AL 35899

<sup>3</sup>Jacobs Sverdrup ESTS Group, Huntsville AL 35812

<sup>4</sup>Carnegie Institution of Washington, Washington DC 20015

<sup>5</sup>NASA-Marshall Space Flight Center, MSFC AL 35812

[cchen@che.uah.edu](mailto:cchen@che.uah.edu)

**Abstract.** Many Lab-on-Chip applications require sample pre-treatment systems. Using electric fields to perform cell lysis in bio-MEMS systems has provided a powerful tool which can be integrated into Lab-on-a-Chip platforms. The major design considerations for electro-lysis devices include optimal geometry and placement of micro-electrodes, cell concentration, flow rates, optimal electric field (e.g. pulsed DC vs. AC), etc. To avoid electrolysis of the flowing solution at the exposed electrode surfaces, magnitudes and the applied voltages and duration of the DC pulse, or the AC frequency of the AC, have to be optimized for a given configuration. Using simulation tools for calculation of electric fields has proved very useful, for exploring alternative configurations and operating conditions for achieving electro cell-lysis. To alleviate the problem associated with low electric fields within the microfluidics channel and the high voltage demand on the contact electrode strips, two "control plates" are added to the microfluidics configuration. The principle of placing the two controlling plate-electrodes is based on the electric fields generated by a combined insulator/dielectric (glass/water) media. Surface charges are established at the insulator/dielectric interface. This paper discusses the effects of this interface charge on the modification of the electric field of the flowing liquid/cell solution.

## 1. Introduction

Many Lab-on-a-Chip applications require sample pre-treatment systems. Using electric fields to perform cell lysis in bio-MEMS systems has provided a powerful tool which can be integrated into Lab-on-a-Chip platforms [1-3]. The major design considerations for electro-lysis devices include optimal geometry and placement of micro-electrodes, cell concentration, flow rates, optimal electric field (e.g. pulsed DC vs. AC), etc. The electric field strength must also be moderated to lyse the cell but at the same time not destroy cell components that are to be studied. To avoid electrolysis of the flowing solution at the exposed electrode surfaces, magnitudes and the applied voltages and duration of the DC pulse, or the frequency of the AC, have to be optimized for a given configuration [2]. Using simulation tools for calculation of electric fields has proved very useful [2-4] for exploring alternative configurations and operating conditions for achieving electro cell-lysis. This paper describes a numerical modelling development of a continuous-flow microfluidic device involving using a pair of control plates to produce desired electric field for cell lysis. The principle of placing the two controlling electrodes is based on the electric fields generated by a combined insulator/dielectric (glass/water) media. In fluid flows, both the permittivity and the conductivity affect the flow [5].

Based on electromagnetic theory [2], surface charges are established at the insulator/dielectric interface. The presence of this interface charge will modify the electric field of the flowing liquid/cell solution. In the next section, we summarized the leaky dielectric/electric field equations and the numerical modelling approach.

## 2. Modelling Approach

### 2.1. Electric Field Equations and Numerical Method

The governing electric current continuity equation for the lysing device is given as:

$$\frac{\partial \rho}{\partial t} + \nabla \cdot \vec{J} = 0 \quad (1)$$

Where  $\rho$  is the charge density and  $\vec{J}$  is current density. Using the Gauss' law and introducing the electric field strength,  $\vec{E}$  and electric potential,  $\varphi$ , we have

$$\frac{\partial}{\partial t} (\nabla \cdot \epsilon \nabla \varphi) + \nabla \cdot (\sigma \nabla \varphi) = 0 \quad (2)$$

Where,  $\epsilon$  is the permittivity and  $\sigma$  is the conductivity of the media. The electric current density is  $\vec{J} = \sigma \vec{E}$ .

For numerical solutions, two separate equations are solved in different regions of the calculation domain such that:

$$\begin{cases} \nabla \cdot \left( \frac{\sigma \Delta t}{\epsilon_0} + \epsilon_r \right) \nabla \varphi^n = \nabla \cdot \epsilon_r \nabla \varphi^0, & \text{conductor regions} \\ \nabla \epsilon_0 \epsilon_r \nabla \varphi = \rho, & \text{dielectric material regions} \end{cases} \quad (3)$$

Where,  $\epsilon_0$  is the permittivity of vacuum;  $\epsilon_r$  is the relative permittivity with  $\epsilon = \epsilon_0 \epsilon_r$ ;  $n$  indicates the solution at the new time step and  $o$  indicates the solution at the previous time step. Sub-iterations are performed at each time step to calculate the electric potential for the new time step. In the absence of an externally specified surface charge density, the conductor-insulator interface condition is a part of the solution, enforced using the jump condition:

$$\left. \frac{\partial \rho_s}{\partial t} \right|_{\text{int,dielectrics-side}} = \nabla \cdot \sigma \nabla \varphi \Big|_{\text{int,conductor-side}} \quad (4)$$

where  $\rho_s$  is the surface charge density at the interface. The implementation for jump condition is the total current from equation (4) across the interface:

$$J^* = \left( \frac{\sigma \Delta t}{\epsilon_0} + \epsilon_r \right) \nabla \varphi^n - \epsilon_r \nabla \varphi^0 \quad (5)$$

Then across the interface of conductor/insulator, we have

$$J^* = \left( \frac{\sigma \Delta t}{\epsilon_0} + \epsilon_r \right) \nabla \varphi^n - \epsilon_r \nabla \varphi^0 = \text{constant} \quad (6)$$

Equation (6) can also be obtained from the first equation in equation (3). This gives us the following discretized equation across the interface:

$$\left(\frac{\sigma\Delta t}{\epsilon_0} + \epsilon_r\right)_c \frac{\phi_f - \phi_c}{\delta n_c} = \left(\frac{\sigma\Delta t}{\epsilon_0} + \epsilon_r\right)_d \frac{\phi_d - \phi_f}{\delta n_d} + \left\{ \epsilon_r E_n^o \right\}_d - \left\{ \epsilon_r E_n^o \right\}_c \quad (7)$$

Where, subscript c, d, and f mean conductor, insulator and interface.  $\delta n_c$  and  $\delta n_d$  are the normal distance from conductor side to interface and insulator side to interface and  $E_n^o$  is the normal electric field strength at previous time step. It is obvious that the last two terms in equation (7) is the surface charge at the interface at the previous time step:

$$\rho_s^o = \left\{ \epsilon_r E_n^o \right\}_d - \left\{ \epsilon_r E_n^o \right\}_c \quad (8)$$

We can solve for interface potential from equation (7):

$$\phi_f = \frac{\left(\frac{\sigma\Delta t}{\epsilon_0} + \epsilon_r\right)_c \cdot \frac{\phi_c}{\delta n_c} + \left(\frac{\sigma\Delta t}{\epsilon_0} + \epsilon_r\right)_d \frac{\phi_d}{\delta n_d} + \rho_s^o}{\frac{1}{\delta n_c} \cdot \left(\frac{\sigma\Delta t}{\epsilon_0} + \epsilon_r\right)_c + \frac{1}{\delta n_d} \cdot \left(\frac{\sigma\Delta t}{\epsilon_0} + \epsilon_r\right)_d} \quad (9)$$

From here, the divergence term of right hand side of equation (3) can be calculated accurately. After applying Gaussian theorem at the interface, the charge accumulated at the interface is calculated:

$$\begin{cases} \epsilon \bar{E} - \epsilon_1 \bar{E}_1 = \rho_{s1} \\ \epsilon \bar{E} - \epsilon_2 \bar{E}_2 = \rho_{s2} \end{cases} \quad (10)$$

Where, E is electric field strength,  $\rho_s$  is surface charge density. 1 refers to the interface with conductor 1 and 2 refers to the interface at conductor 2. The above are the basic formulation for the E-field calculations in the combined materials. The formulation includes time-domain calculations of the electric field and currents in the material. The above numerical method was incorporated into CFD-ACE+ [8] for the electric field calculations.

## 2.2 The Microfluidics Cell Lysis Device

A simple microelectrode geometry as shown in figure 1(a) was the starting point of constructing a continuous-flow device. In the figure, also shown in figure 1(b) for the cross-section view, high voltage platinum micro-strips are placed

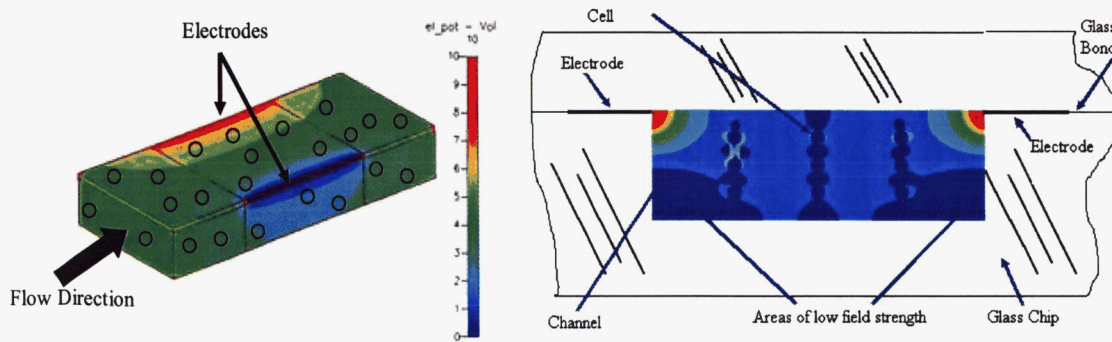


Figure 1 (a), Basic microfluidic channel with electrodes; (b), Cross section of the electro-lysis channel with thin electrodes adjacent to the liquid.

on the top edge of the channel. Figure 1(b) shows the electric field when 10V DC is applied across the two electrodes. It can be seen that at the two lower corners, the field strength reduces to much lower level (less than  $10^5$  V/m). Depending on the cell type, field strength greater than  $3 \times 10^5$  V/m [3, 4, 7] should be maintained for cell lysis.

To alleviate the problem associated with low electric fields within the microfluidics channel and the high voltage demand on the contact electrode strips, two "control plates" are added to the microfluidics configuration. These two plates are placed at about 500 micro meters above and below the channel. The theoretical background for placing the two controlling electrodes is based on the electric fields generated by a combined insulator/dielectric (glass/water) media. In fluids, both the permittivity and the conductivity affect the flow [5]. Based on electromagnetic theory [6], surface charges are established at the insulator/dielectric interface. Based on the numerical modelling results, this surface charge and the electrical double layer established will generate sufficient electric field (perpendicular to the electric field generated by the lysing electrodes) at the corner regions. The suggested operating conditions summarized below are based on the conductivity of the dielectric media (water), as well as relative permittivity of both insulator (glass/SiO<sub>2</sub>) and dielectric material (water). Several operating methods are possible. For example, either AC or square pulses [1,2] can be applied at the electrodes. To avoid water electrolysis [2], AC was used in this analysis. Due to the large difference in time constants (estimated from the ratio of permittivity and conductivity), a DC was applied across the control plates. Here we present the results of AC of 20V across the electrodes and a constant 400V across the control plates. The AC was simulated as a cosine wave with 0.1MHz. In figure 2, the electric field magnitudes are shown at the beginning of the cycle (2.a) and at the half cycle (2.b). It can be observed that the low-strength areas at the two lower corners have been much reduced. In figure 3, the surface charges at both top and bottom channel walls are plotted at the beginning, at  $\frac{1}{4}$ , and at half of the AC cycle.

### 3. Concluding Remarks

In this study, we have utilized a numerical simulation tool to investigate the design of a continuous microfluidics based cell lysis device. Original lysing channel configuration with two thin electrode strips wall-flushed at both upper portion of the channel creates low electric field outside of "kill zone" [4] at lower portion of the channel. The proposed new configuration by incorporating a pair of control plates placed above and below the channel has shown its effectiveness in increasing the electric field strength. Comparison with experimental testing is currently underway to verify the proposed operating conditions.

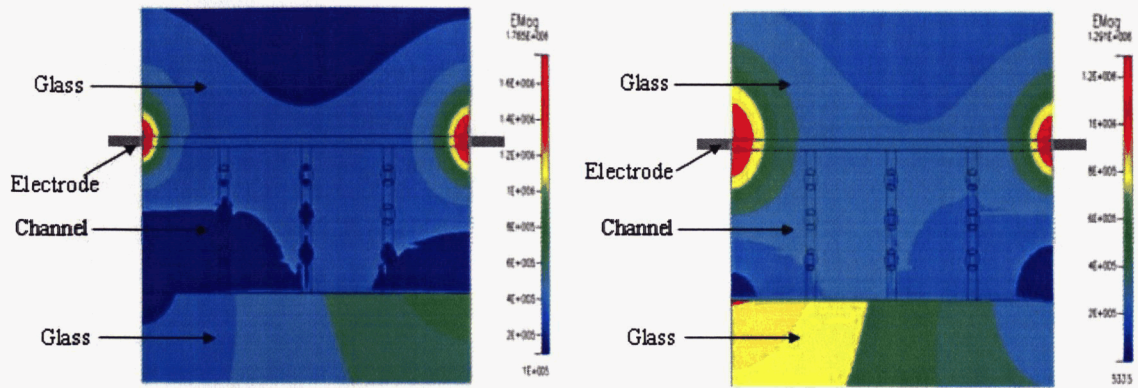


Figure 2. Cell lysis channel with control panels (two panels above and below the channel not shown); (a) electric field magnetite at the beginning of the cycle, (b) at half cycle.

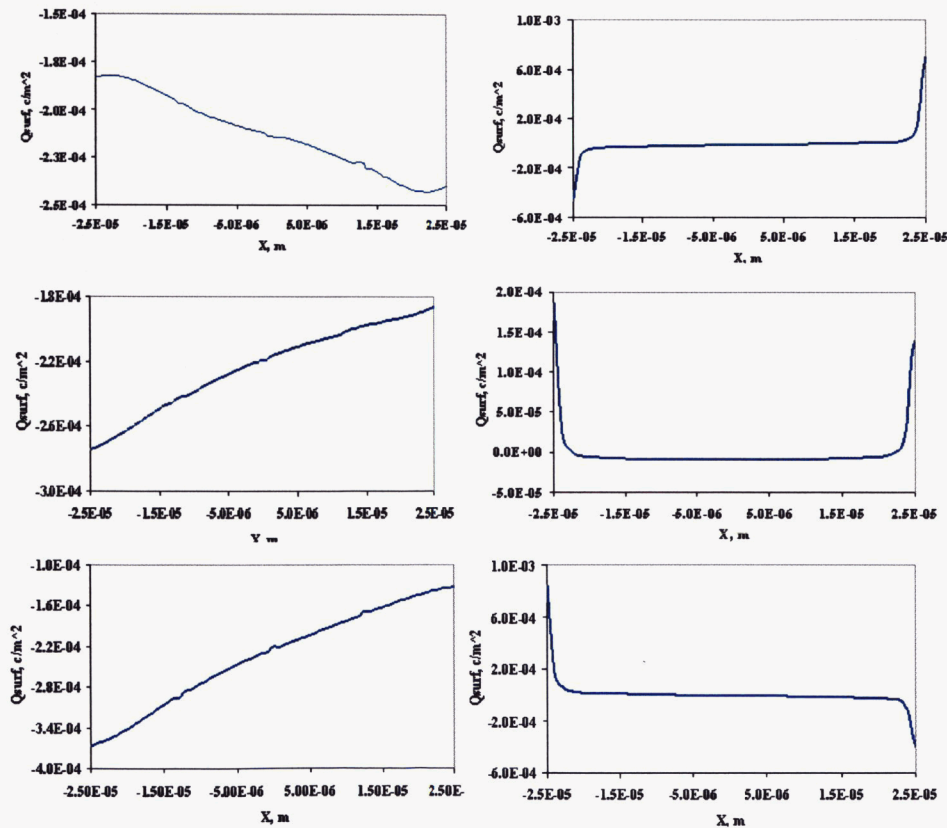


Figure 3. Surface Charges at the top wall (left column) and bottom wall (right column) of the microchannel; (a) at the beginning of the cycle (top row), (b) at quarter cycle (middle row), (c) at half cycle.

## Acknowledgements

The Authors are grateful for the funding of this work via the LOCAD project through the Exploration Science and Technology Directorate at Marshall Space Flight Center. Technical consultation on the time-domain method from Dr. Z. J. Chen of CFDRC is acknowledged.

## References

- [1] Lee, S.-W. and Tai, Y.-C., "A micro cell lysis device," *Sensors and Actuators A: Physical*, 73, 74-79, 1999.
- [2] Lu, H., Schmidt, M. A. and Jensen, K. F., "A Microfluidic Electroporation Device for Cell Lysis," *Lab on a Chip*, 5, 23-29, 2005.
- [3] Ramadam, Q., Samper, V., Poenar, D., Liang, Z., Yu, C. and Lim, T. M., "Simultaneous Cell Lysis and Bead Trapping in a Continuous Flow Microfluidic Device," *Sensor and Actuator B*, vol. 113, pp. 944-955, 2006.
- [4] Oakley, B., de Hagen, J. Hanna, D., Al-Khateeb, B. and Al-Nsour M., "Simulation of Electromagnetic Fields in a Microelectrode Array," Proc. IEEE EMBS Special Topic Conf. Molecular and Cellular Tissue Engineering, Genova, Italy, 2002.
- [5] Saville, D. A., "Electro-hydrodynamics: The Taylor-Melcher Leaky-dielectric Model," *Annu. Rev. Fluid Mech.*, Vol. 29, pp. 27-64, 1997.
- [6] Shen, L. C. and Kong, J. A., *Applied Electromagnetism*, 3<sup>rd</sup> ed., PWS Publishers, 1995.
- [7] Miklavcic, D., Semrov, D., Mekid, H and Mir, L. M., "In vivo Electroporation Threshold Determination," Proc. 22<sup>nd</sup> Annual EMBS International Conference, Chicago, IL., July 23-28, 2000.
- [8] CFD-ACE+, ESI-Group, North America, Huntsville, 2006.